Growth of Nanocolumnar Thin Films on Patterned Substrates at Oblique Angles

A. Garcia-Valenzuela[1], S. Muñoz-Piña[2], G. Alcala[2], R. Alvarez[1,3*], B. Lacroix[4,5], A. J. Santos[4,5], J. Cuevas-Maraver[3,6], V. Rico[1], R. Gago[7], L. Vazquez[7], J. Cotrino[1,8], A.R. Gonzalez-Elipe[1], A. Palmero[1*]

[1] Instituto de Ciencia de Materiales de Sevilla (CSIC-Univ. Sevilla). Avda. Américo Vespucio 49. 41092, Seville, Spain

[2] Universidad Complutense de Madrid, Dep. Ingeniería Química y de Materiales, Avenida Complutense s/n, Facultad de Ciencias Químicas, 28040 Madrid, Spain

[3] Departamento de Física Aplicada I. Escuela Politécnica Superior, Universidad de Sevilla. c/ Virgen de África 7, 41011, Seville, Spain

[4] Departamento de Ciencia de los Materiales e Ingeniería Metalúrgica y Química Inorgánica, Universidad de Cádiz, Campus Universitario Río San Pedro s/n, 11510, Puerto Real (Cádiz), Spain

[5] Instituto de Microscopía Electrónica y Materiales (IMEYMAT), Universidad de Cádiz, Spain

[6] Instituto de Matemáticas de la Universidad de Sevilla (IMUS). Edificio Celestino Mutis. Avda. Reina Mercedes s/n, 41012-Sevilla, Spain

[7] Instituto de Ciencia de Materiales de Madrid (CSIC), E-28049 Madrid, Spain

[8] Departamento de Física Atómica, Molecular y Nuclear, Universidad de Sevilla, Avda. Reina Mercedes s/n. E-41012 Seville, Spain

Abstract

The influence of one dimensional substrate patterns on the nanocolumnar growth of thin films deposited by magnetron sputtering at oblique angles is theoretically and experimentally studied. A

well-established growth model has been used to study the interplay between the substrate topography and the thin film morphology. A critical thickness has been defined, below which the columnar growth is modulated by the substrate topography, while for thicknesses above, the impact of substrate features is progressively lost in two stages; first columns grown on taller features take over neighboring ones, and later the film morphology evolves independently of substrate features. These results have been experimentally tested by analyzing the nanocolumnar growth of SiO_2 thin films on ion-induced patterned substrates.

Email: rafael.alvarez@icmse.csic.es; alberto.palmero@csic.es

Introduction

Nanocolumnar porous thin films deposited at oblique geometries are nowadays receiving much attention due to their unique morphological features and remarkable properties.[1] While their high specific surface can be exploited for the development of gas or liquid sensor devices,[2-4] the possibility to fine tune their density[5] and connectivity among pores[6-7] make them also suitable for other applications in technological fields such as biomedicine, plasmonics, microfluidics, batteries or photonics, among others.[8-13] In all these cases, the relevant specific features of the nanocolumnar structures (e.g. their size, tilt, average distance, anisotropic distributions, preferential direction of coalescence, etc.) are intimately connected to the governing growth mechanisms. In this regard, the surface shadowing phenomenon emerges as a key nanostructuration process mediating the formation of nanocolumns with typical diameters in the order of few tens of nanometers.[14-15] This mechanism takes place whenever gaseous deposition species arrive at a substrate along a preferential oblique direction, whereby taller features on the film surface inhibit the deposition in neighbor regions, giving rise to different nanocolumnar arrays.[16]

From an experimental point of view, porous nanocolumnar thin films have been classically grown by evaporating a given material in vacuum and promoting the glancing incidence of gaseous deposition species onto a tilted substrate, in a so-called Glancing Angle Deposition.[1] Yet, and due to difficulties to upscale this technique to typical industrial standards,[17] other alternatives have been analyzed to achieve nanocolumnar structures.[18] Among them, the magnetron sputtering technique operated at oblique angles (MS-OAD), also called magnetron sputtering at glancing angles (MS-GLAD), has emerged as one of the most interesting procedures in terms of efficiency, reliability, reproducibility and potential industrial scalability. It relies on the interaction of a plasma and a solid

target to vaporize atomic species from the latter that, emitted preferentially in the normal direction with respect to its surface, are subsequently deposited on a substrate.[19] In this way, when the substrate is tilted with respect to the target, sputtered species may arrive along a preferential oblique direction.[20] In the last decade, MS-OAD has managed not only to reproduce similar film morphologies as those classically obtained by the evaporation technique, but also to widen its possibilities. For instance, in refs. [21-22], we studied the influence of some experimental controllable parameters (e.g. deposition pressure, tilt angle of the substrate, ion impingement, etc.) on the film morphology, finding different tilted nanocolumnar structures with mass densities ranging from 100% to near 30% with respect to the compact layer, or even sponge-like vertically-aligned coalescent structures.

The variety of typical porous morphologies that can be achieved by MS-OAD is rich, permitting the customization of film nanostructures with optimum performance in numerous functional applications (see for instance [23-25]). However, to our knowledge, there are important unexplored conditions that require further study and that might widen the possibilities of the method even more. For instance, in ref. [26] we demonstrated that when a thin porous layer is grown on top of a rough nanocolumnar film, the former reproduces the surface features of the latter, in a so-called structural propagation phenomenon, which is of special relevance when growing periodic multilayer structures (e.g. photonic crystals or Bragg reflectors).[9] On the other hand, and even though there has been an increasing amount of publications dealing with the influence of substrate features on the film growth (see for instance [27-30]), to our knowledge, no general framework analyzing the interplay between both has been put forward yet. In this paper we aim at developing such framework by studying how substrate features may affect the film nanostructure when using the MS-OAD technique. In particular, we focus on the effect of one dimensional quasi-periodic patterned substrates, characterized by peak-to-peak distances in the order of few hundred

nanometers, very similar to those experimentally obtained by ion beam sputtering.[31-39] To address this problem, we have first used a well-accepted model to theoretically simulate and analyze the growth of a thin film on purely periodic and near periodic patterned substrates at oblique angles and, subsequently, experimentally test these results by analyzing the growth of porous SiO_2 thin films on quasi-periodic ion-induced patterned Si substrates. We have chosen this particular film composition because it is a well-known material, whose properties have been widely studied in the literature. However, our aim is general and our results can be easily extrapolated to more general conditions and other materials. Based on this analysis, relevant general conclusions can be achieved on the influence of substrate features on the structural development of porous nanocolumnar thin films.

Growth Model

The growth model has already been described in detail in refs. [21, 40] and references therein, where it was proven adequate to describe the growth of numerous materials by MS-OAD in the absence of ion bombardment and at low temperatures, i.e. in the so-called zone I of the Thornton Structure Zone Model.[41-42] We describe it here, although for further details refs. [21, 40] are recommended. The model considers the deposition of Si effective particles on a cubic three-dimensional $N_L x N_L x N_H$ grid with periodic boundary conditions, whose cells may take the values 0 (empty cell) or 1. Each cell represents a Si atom in the network that becomes fully oxidized once it is deposited. Thus, the size of each cell is assimilated to the typical volume of a SiO_2 molecule in the material (i.e., a typical length of ~0.5 nm). A number of deposition particles per unit time and unit surface are thrown towards the substrate from an initial random position above the film, following

the direction defined by an incident angle distribution function. This distribution is calculated as a function of the experimental conditions (reactor geometry, tilt angle of the substrate and other geometrical constrains) by the widely accepted SIMTRA code.[43-44] This software describes the collisional transport of sputtered species through the plasma gas by means of binary collisions. The angle and energy distribution of sputtered species at the target are calculated by the software SRIM, [45] which is typically used to describe the ion-assisted sputtering process. An average gas temperature of 350 K and a screened Coulomb potential (Molière type) were considered in the simulations under the assumption of a circular racetrack with a radius of 2 cm. We have run our simulations in small scales (N_L and N_H up to 2000 cells) to first analyze the general dependence between substrate features and the morphology of the film, and subsequently extrapolate the results to comply with the larger spatial scales of the experimental data (in the order of few microns).

Experimental Details

Quasi-periodic patterned Si substrates were prepared by irradiation with 500 eV Ar^+ ions as described in ref. [46]. Depending on the irradiation conditions, this technique allows the formation of different patterns on the substrate, from surface ripples to elongated islands.[33] The ion beam was extracted from a broad beam Kaufman ion source (3 cm) at a base and working pressures of $5x10^{-4}$ and $2x10^{-2}$ Pa, respectively, and impinged on the substrates at an incidence angle of 75º with respect to the surface normal. The experiments were performed for an average current density on the target of 300μA/cm^2 and an ion dose of $2.3x10^{18}$ ions/cm^2 (irradiation time was 240 minutes). The target was water-cooled during the irradiation, reaching a temperature of 30ºC.

A set of amorphous SiO_2 thin films were grown on the patterned substrates using reactive MS-OAD. A 3 in. diameter Silicon target was employed for the depositions, placing the substrate holder at a distance of 7 cm and a discharge power of 200 W. Deposition time in each case was chosen to grow films with thicknesses between 200 and 3000 nm, as determined by means of cross-sectional Field Emission Scanning Electron Microscopy (FESEM) images. The base pressure of the deposition reactor was $7x10^{-4}$ Pa. The argon and oxygen partial pressures during depositions was kept at 0.2 and 0.05 Pa, respectively, which was enough to operate in the oxidic mode of the discharge and get fully oxidized films.[19] Samples were prepared simultaneously on flat and patterned substrates, tilting them 80º (see figure 1).

The morphology of the SiO_2 nanocolumns from the film surface to the substrate was studied by transmission electron microscopy (TEM) at the scientific integrated services (SC-ICYT) of the University of Cádiz (Spain). High-angle annular dark-field (HAADF) imaging of the sample was performed in a 200 kV JEOL 2010F microscope using the scanning TEM (STEM) mode with a probe size of about 1 nm. Prior to observation, cross-sectional specimens were prepared using the flat-type tripod polishing approach in order to thin the sample down to a few micrometers, followed by a final ion milling step with 3-3.5 keV Ar^+ ions up to electron transparency.

The surface topography of the substrates and films were imaged by atomic force microscopy (AFM). The measurements were performed in the non-contact dynamic mode with a Nanoscope IIIa equipment (Veeco@) and with PicoPlus 5500 (Agilent). Silicon cantilevers with nominal tip radius of curvature of 8 nm were used. Images were composed of 512 x 512 up to 2048 x 2048 pixels. FESEM pictures were also recorded for each film using a Hitachi S4800 microscope at the Instituto de Ciencia de Materiales de Sevilla (CSIC-US, Seville, Spain). The surface roughness, w, and correlation length, l, of the samples were obtained using the Gwyddion freeware package[47] using the formula

$$w = \sqrt{\int dxdy\,[z(x,y) - \bar{z}]^2/\mathrm{S}},$$

where x and y denote the position coordinates of the substrate, S the surface area under analysis, z the height of the film and $\bar{z}$ the mean height. Moreover, l has been calculated along the x axis (see figure 1) by obtaining the first minimum, r_0, of the (one dimensional) height-height correlation function, h, as a function of the distance, r, defined as

$$h(r) = \int dxdydx'dy'(z(x,y) - \bar{z})(z(x',y') - \bar{z})\,/w^2\,,$$

with $r = |x - x'|$ and $y = y'$. In this way, the surface correlation length is defined as $l = 2r_0$.

Simulation analysis

To illustrate the results of the simulations we first assume that the patterns possess a typical sinusoidal shape in the xy plane defined as $z_s(x,y) = A[1 + sin(2\pi x/\lambda)]$, where z_s is the substrate height, λ the wavelength and A the amplitude of the ripples. For this surface topography, the correlation length of the substrate in the x direction, l_s, is $l_s = \lambda$, and the surface roughness of the substrate, w_s, is $w_s = A/\sqrt{2}$. We have performed different simulations for values of λ and A up to λ=500 and A=50cells. In figure 2a we illustrate the results by showing the cross-sectional views of four generic cases, when λ=80 and 160 cells and A=5 and 25 cells. There, different columnar arrangements are visible depending on substrate features, from which three important conclusions can be drawn: i) the column tilt angle is rather independent of the substrate features, ii) each column grows on top of a ripple, and iii) column diameter strongly depends on λ and very weakly on A. These three main evidences stem from the fact that surface shadowing promotes the growth of taller surface features over lower ones and thus induces that a column grows on top of each ripple,

depicting a tilt angle and diameter that mainly depends on the incident angle distribution of deposition particles and not on any specific substrate feature.[1, 16]

In order to further analyze the columnar growth, in figure 2b we also show the evolution of l as a function of film thickness, Δ. In this way, for small film thicknesses, the relation l=l_s is fulfilled, i.e. the film grows following the arrangement of the ripples. Yet, when Δ reaches a certain critical threshold, the correlation length departs from this value, implying that the typical correlation distances over the film surface do no longer follow that of the ripples. Due to its importance in this work, we dub this thickness *oblivion thickness*, Δ_O. Moreover, according to figure 2b, when $\Delta > \Delta_O$, the curve converges to that of a film deposited on a flat surface (also shown in figure 2b), i.e. the film growth becomes independent of substrate features. A similar analysis can be performed regarding the evolution of the surface roughness, also depicted in figure 2b. Remarkably, and despite the different original roughness of the substrates, w increases with Δ when $\Delta < \Delta_O$, mainly due to the preferential development of the columns on top of the ripples. This trend continues until the valleys between columns are no longer visible from the top, decreasing or reaching a plateau for $\Delta \gtrsim \Delta_O$, when the roughness values converge to those of a film grown on a flat substrate.

The two growth regimes described above are illustrated in figure 3, where we show top views of simulated films using flat and periodic rippled substrates (case with $\lambda = 80$ and $A = 25$ cells) for three values of Δ. There, it is apparent that columns arrange according to the ripple pattern when $\Delta < \Delta_O$. However, when $\Delta \gtrsim \Delta_O$ the pattern starts to vanish until, for $\Delta \gg \Delta_O$, the film surface looks very similar to that of a film grown on a flat substrate. In figure 4 we show the calculated values of Δ_O as a function of A and λ, finding a weak and strong dependence on these two parameters, respectively. This relation can be understood as an outcome of a shadowing dominated growth, by which the taller a surface feature is the more species are deposited on it, rapidly amplifying any initial surface protuberance. Hence, a surface with small ripple amplitudes would develop similarly

to another with larger ones, as long as these are spatially distributed similarly. Interestingly, we have found a clear relation between Δ_O and λ as a power law in the studied spatial range,

$$\Delta_O \propto \lambda^{\gamma}, \tag{1}$$

with $\gamma = 1.55 \pm 0.04$. Once we have analyzed the growth of thin films when the patterns follow well-defined periodic ripples, we analyze more realistic situations when λ and A are allowed to fluctuate around average values. We have therefore carried out the same analysis as before but assuming variations of λ and A over the averaged values $\langle\lambda\rangle = 80$ and $\langle A\rangle = 25$ cells, with a dispersion of 25%. The cross-sectional views of these films in figure 5a show how fluctuations in λ lead to a columnar growth similar to that of the purely periodic case: the value of l as a function of Δ appears in figure 5b which yields $l = \langle\lambda\rangle$ in the initial stages of growth, departing from this behavior at a similar oblivion thickness as in the purely periodic substrate case. The top view of this film for different values of Δ, reported in figure 3, corroborate the similarities between both cases. Figures 5a-b report the simulation results when A fluctuates and show that the development of the film nanostructure drastically changes from the previous cases: after an initial development defined by the relation $l = \langle\lambda\rangle$, a new growth stage emerges. In this new stage, columns grown on taller mounds take over neighboring ones suppressing their growth, in agreement with a well-known phenomenon associated to the shadowing mechanism and the abovementioned preferential growth of taller features over lower ones.[1, 16] This columnar cannibalization process ends up with the formation of tilted thick structures that introduce a new correlation length over the film surface, as evidenced in figure 5b. Once these structures are formed, for large film thicknesses, l evolves parallel to that of a film grown on a flat surface, i.e. the growth is equivalent to that of a thicker film deposited on a flat substrate. Same behavior can be found regarding the surface roughness evolution of the films, also depicted in figure 5b.

According to the discussion above, three stages of growth are found as a function of thickness when the amplitude of the substrate ripples is allowed to fluctuate:

i) A *Substrate-driven* (SD) growth when $\Delta < \Delta_o$, similar to that appearing in the pure periodic case, where a column grows on top of each ripple with $l = \langle\lambda\rangle$ (see figure 3). This type of growth dominates the morphological development of the film until the thickness reaches the oblivion point. In this regard, Δ_o shows now a strong dependence on both, the wavelength and the amplitude fluctuations of the ripple pattern, and results in a lower value than in the absence of amplitude fluctuations. Under these conditions, the calculated trend in eq. (1) must be understood as an upper bound for the actual oblivion thickness.

ii) A *Columnar Aggregation* (CA) stage when $\Delta \gtrsim \Delta_0$, in which taller columns take over surrounding ones and form large tilted structures. These structures introduce a new correlation length over the surface and evolve with thickness very differently to those obtained on a flat substrate (see figure 3).

iii) A *Free Growth Stage* (FG) when $\Delta \gg \Delta_0$, in which the film grows independently of the substrate feature (see figure 3).

To complete this analysis, we have included the results of the simulations when both λ and A fluctuate in figure 5b, finding a similar trend than that when only A fluctuates.

Experimental Results and Discussion

In the previous section we have studied the phenomenology when the films grow on periodic and quasi-periodic patterned substrates. Among all the cases studied, the most relevant one corresponds to that when the amplitudes were allowed to fluctuate: this case did not only show a characteristic phenomenology that includes all relevant effects present in the remaining two situations under study, but also introduced new phenomena regarding the columnar growth. That is why, from an experimental point of view, we have focused on this particular problem and used a patterned substrate containing fluctuations in amplitude and wavelengths to test the theoretical framework developed in the previous section.

In figure 6 we show the topography of an as-prepared patterned substrate, measured by AFM, along with a cross sectional height profile along the direction defined by the arrow. The analysis of this surface map yields values of roughness and correlation length of $w_s \sim 32$ nm and $l_s \sim 550$ nm, respectively. As described in the Experimental Details section, we have simultaneously deposited SiO_2 thin films on patterned and flat substrates. Deposition was carried out at oblique geometries with particle incidence in the direction of the arrow in figure 6. For the sake of clarity, from now forth we label the film grown on a flat substrate with the format "F-film thickness", whereas the film grown on a patterned substrate will be labeled as "P-film thickness". In figure 7a we show the top SEM images of the two substrates and those of F-380 nm and P-380 nm films. These two latter cases present profound differences: while a typical granular surface topography is found in the former type of films, the latter shows larger nanostructures that retain the distribution pattern of substrate features. This is more evident in figure 7b, where the calculated correlation length indicates that for the sample P-380 nm, the relation $l = l_s$ holds, i.e. the columns follow the substrate pattern, while for sample F-380 nm the correlation length is much shorter. This implies that for P-380 nm film, the

substrate features have modulated the morphological evolution of the film in a typical SD growth regime. Here is important to mention that due to the fluctuating nature of the heights defining the substrate in different spatial scales (see top image in figure 6), the development of the film does not follow every minor detail on the substrate, but only those that are tall enough to define the correlation length, and that will serve as nucleation sites for the subsequent columnar development. This mound-selection mechanism, by which the growth of small surface protuberances becomes inhibited in favor of larger ones, is present in this type of depositions since early stages of growth.[1]

Differences are more pronounced when the film thickness is 640 nm: as expected, the F-640 nm film in figure 7a shows a similar morphology than the F-380 nm case, but with larger grains. Remarkably, the P-640 nm film surface strongly differs from that of the P-380 nm film and is characterized by numerous piled up slices of material that appear aligned with the original substrate patterns. Indeed, this morphology defines a new correlation length and suggests that the substrate pattern effect is vanishing from the film surface. This is corroborated in figure 7b, where the relation $l > l_s$ for P-640 means that Δ_o should stay between 380 and 640 nm, below the estimated value for a pure periodic substrate (figure 5), above ~1800 nm, as deduced from our simulations and the discussion above. This is evident regarding the cases P-1000, P-2000 nm and P-3000 nm, where we appreciate that i) the slices of material have disappeared, and ii) a mounded topography is now evident in all these cases, with grain size much larger than those appearing on the films grown on flat substrates. This latter result is more evident in figure 7b, where we see that the correlation lengths of P-1000 nm, P-2000 nm and P-3000 nm follow a trend parallel to that of the films deposited on flat substrates, implying that the growth is equivalent to that of a ~3.5 μm thicker film deposited on a flat substrate (see figure 7b for details). The analysis on the roughness evolution, also shown in figure 7b, yields similar conclusions.

In order to further illustrate the differences between the films grown on flat and patterned substrates, in figure 8a we show a cross-sectional SEM image of the P-1000 nm film, where we notice the good agreement between the calculated tilt angle of the columns and the experimental value (~35º in both cases), corroborating the adequacy of the simulations. Moreover, the STEM-HAADF image of a 3 μm thick film grown on a patterned substrate is shown in figure 8b (note that plane of cut is not the same than in figure 8a). There, it is apparent an intrinsic relation between substrate mounds and the appearance of columns, which only seems to grow on top of medium and large-size surface protuberances. Remarkably, in figure 8b it is also apparent that at heights between ~500 and ~1000 nm some columns are incorporated onto larger columnar structures (note that for larger thicknesses some columns have also been removed when polishing the sample for the STEM-HAADF measurement). This is also in agreement with the simulation results on the influence of patterns on the film growth where, for this range of thickness, we demonstrated the existence of a CA regime where columns on taller mounds take over neighboring ones, forming large tilted structures. From figure 8b, this means that Δ_0 in this case should be around 500 nm, in agreement with our discussion above. Finally, once these larger tilted structures are formed (for film thicknesses above ~1000 nm), they grow homogeneously in a FG regime. These results corroborate our discussion above on the existence of an oblivion thickness and on the existence of three stages of growth as a function of thickness.

The generalization of our results to more complex situations, e.g. when using two dimensional patterned substrates, is not straightforward, although it seems plausible that the obtained growth regimes could anisotropically emerge depending on the complexity of the pattern. Therefore, and even though this paper has focused on the growth of nanocolumns on patterned substrates, some generic conclusions can be extrapolated to numerous situations where these substrates contain patterns whose characteristic length or amplitude fluctuate. For instance, our results suggest that

the intrinsic roughness of (non-polished) substrates could have a strong impact on the film morphology, especially when any surface height correlation might define a characteristic wavelength with fluctuating amplitude. In this case, it is likely that the columnar development is strongly affected by substrate features. Moreover, our results also explain the structural propagation mechanism when growing thin porous layers on top of a rough surface, by which the growth of the former tend to follow the features of the latter.[26] Under the light of our results, this issue arises when the thickness of each porous monolayer is below the oblivion thickness, which imposes a dependence between its morphology and that of the surface below.

Conclusions

In this paper we have analyzed the influence of substrate patterns on the nanocolumnar development of thin films grown by magnetron sputtering at oblique angles. For this, we have firstly made a simulation analysis on how the amplitude and the wavelength of the substrate pattern affect the morphological evolution of the films, finding that i) the column tilt angle is rather independent of the substrate features, ii) columns seem to grow on top of each seed in the studied spatial range, and iii) column diameter strongly depends on the substrate wavelength and weakly on the amplitude. Moreover, for low film thicknesses we have obtained that columns tend to arrange following the substrate features, in a Substrate Driven growth mode, while for higher thicknesses there is a critical thickness, the so-called oblivion thickness, above which the information on the substrate features is progressively lost. This process takes place through two well differentiated phases for increasing film thicknesses: a first one, dubbed Columnar Aggregation stage, in which columns grown on taller features take over neighboring ones and form large tilted structures, and a second one, where the film morphology evolves independently of substrate features, in a so-called

Free Growth regime, where the growth is equivalent to that of a thicker film deposited on a flat substrate.

The theoretical framework developed herein has been experimentally tested by performing numerous depositions on flat and ion-induced patterned substrates with height variations, finding an overall good agreement between theory and experiments. Indeed, three growth regimes have been identified, finding a Substrate Driven growth for thicknesses below ~500 nm, a Columnar Aggregation regime for thicknesses between ~500 and ~1000 nm, and a Free growth for thicknesses above ~1000 nm. In this regard, the obtained results do not only explain the influence of substrate features on the film morphology as a function of thickness, but also indicate the importance of the substrate roughness and correlation length on the film characteristics.

Acknowledgements

We acknowledge the support of the University of Seville (VPPIUS and VI PPIT-US), the European Development Funds program (EU-FEDER), and the Spanish Ministry of Economy and Competitiveness and Agencial Estatal de Investigación (AEI) (projects MAT2013-40852-R, MAT2016-79866-R, MAT2015-69035-R, 201560E055, and MAT2015-69035-REDC and MAT2017-85089-C2-1-R), and the Comunidad Autónoma de Madrid (S2013/MIT-3029, NANOAVANSENS, IND2017/IND-7668).

Keywords

Nanostructures; Thin Films; Oblique Angle Deposition; Magnetron Sputtering; Patterned Substrate.

References

[1] A. Barranco, A. Borras, A. R. Gonzalez-Elipe, A. Palmero, Prog. Mater. Sci. **2016**, 76, 59.

[2] X. Xu, M.A.P. Yazdi, J.B. Sanchez A. Billard, F. Berger, N. Martin, Sensors and Actuators B-Chemical **2018**, 266, 773-783.

[3] C. Charles, N. Martin, M. Devel, Surf. Coat. Technol. **2015**, 276, 136-140.

[4] M.S. Rodrigues, D. Costa, R.P. Domingues, M. Apreutesei, P.Pedrosa, N. Martin et al. Applied Surface Science **2018**, 438, 74-83.

[5] S. Liedtke, C. Gruener, J.W. Gerlac, B. Rauschenbach, Belstein Journal of Nanotechnology **2018,** 9, 954-962.

[6] K. Kim, J.H. Park, H. Kim, J.K. Kim, E.F. Schubert, J. Cho, Appl. Phys. Letters **2016**, 108(4), 011910.

[7] V. Godinho, P. Moskovkin, R. Alvarez, J. Caballero-Hernández, R. Schierholz, B. Bera, J. Demarche, A. Palmero, A. Fernández and S. Lucas, Nanotechnology **2014**, 25, 355705.

[8] J. Ollitrault, N. Martin, J.Y. Rauch, J.B. Sanchez, F. Berger, Materials Letters **2015**, 155, 1-3.

[9] M. Oliva-Ramirez, L. Gonzalez-Garcia, J. Parra-Barranco, F. Yubero, A. Barranco and A.R. Gonzalez-Elipe, ACS Appl. Mater. Interfaces **2013**, 5, 6743–50.

[10] C. Sengstock, M. Lopian, Y. Motemani, A. Borgmann, C. Khare, P.J.S. Buenconsejo, T.A. Schildhauer, A. Ludwig, M. Koller, Nanotechnology **2014**, 25, 195101.

[11] Y.J. Yoo, J.H. Lim, G.J. Lee, K.I. Jang, Y.M. Song, Nanoscale **2017**, 9(9), 2986-2991.

[12] L. Yang, Y. Zhao, Y. Feng, J.S. Shan ; X.Y. Liang , J. Huang, J.H. Mi, L.J. Wang, W.M. Shi, Applied Surface Science **2016**, 363, 252-258.

[13] D.B. Polat, O. Keles, Thin Solid Films **2015**, 589, 543-550.

[14] C.Y. Song, G.K. Larse, Y.P. Zhao, Appl. Phys. Letters **2013**, 102(23), 233101.

[15] D. Toledano, R.E. Galindo, M. Yuste, J.M. Albella, O. Sanchez, J. Appl. Phys. **2013**, 46(4), 045306.

[16] T. Karabacak, J.P. Sing, Y.P. Zhao. G.C. Wang, T.M. Lu, Physical Review B **2003**, 68(12), 125408.

[17] R. Alvarez, J.C. Gonzalez, J.P. Espinos, A. R. Gonzalez-Elipe, A. Cueva, F. Villuendas, Applied Surface Science **2013**, 268, 507.

[18] P. Romero-Gomez, A. Palmero, T. Ben, J. G. Lozano, S. I. Molina and A. R. González-Elipe, Physical Review B **2010**, 82, 115420.

[19] Reactive Sputter Deposition, D. Depla, S. Mahieu (Eds.), Springer Series in Materials Science, Springer-Verlag, Berlin, Heildelberg, **2008**. ISBN 978-3-540-76662-9.

[20] R. Alvarez, J. M. Garcia-Martin, M.C. Lopez-Santos, V. Rico, F.J. Ferrer, J. Cotrino, A. R. Gonzalez-Elipe, A. Palmero. Plasma Processes and Polymers **2014**, 11, 571-576.

[21] R. Alvarez, J.M. Garcia-Martin, A. Garcia-Valenzuela, M. Macias-Montero, F.J. Ferrer, J. Santiso, V. Rico, J. Cotrino, A.R. Gonzalez-Elipe, A. Palmero, J. Phys. D: Appl. Phys. **2016**, 49(4) 45303.

[22] M. Macias-Montero, F.J. Garcia-Garcia, R. Alvarez, J. Gil-Rostra, J.C. Gonzalez, J. Cotrino, A.R. Gonzalez-Elipe, A. Palmero, Journal of Applied Physics **2012**, 111(5), 054312.

[23] T. Fujii, Y Aoki, H. Habazaki, Langmuir **2011**, 27(19), 11752-11756.

[24] R.L. Rodriguez-Suarez, L.H. Vilela-Leao, T. Bueno, A.B. Oliveira, J.R.L. de Almeida, P. Landeros, S.M. Rezende, A. Azevedo, Physical Review B **2011**, 83(22), 224418.

[25] K.R. Khedir, G.K. Kannarpady, H. Ishihara, J. Woo, C. Ryerson, A.S. Biris, Langmuir **2011**, 27(8), 4661-4668.

[26] A. Garcia-Valenzuela, C. Lopez-Santos, R. Alvarez, V. Rico, J. Cotrino, A.R. Gonzalez-Elipe, A. Palmero, Nanotechnology **2017**, 28, 465605.

[27] K. Chen, R. Frömter, S. Rössler, N. Mikuszeit and H.P. Oepen, Phys. Rev. B **2012**, 86, 064432.

[28] M. Körner, K. Lenz, M.O. Liedke, T. Strache, A. Mücklich, A. Keller, S. Fracsko, J. Fassbender, Phys. Rev. B **2009**, 80, 214401.

[29] M.O. Liedke, M. Körner, K. Lenz, M. Fritzche, M. Rankan, A. Keller, E. Cizmar, A.A. Zvyagin, S. Facsko. K. Potzger, J. Lindner, J. Fassbender, Phys. Rev. B **2013**, 87, 024424.

[30] A. Keller, L. Peverini, J. Grenzer, G. J. Kovacs, A. Mücklich, S. Facsko, Phys. Rev. B **2011**, 84, 035423.

[31] T. Luttrell, M. Batzill, Phys. Rev. B **2010**, 82, 035408.

[32] M. Kolmer, A.A. Zebari, M. Goryl, F. B. Mongeot, F. Zasada. W- Piskorz, P. Pietrzyk, Z. Sojka, F. Krok, M. Szymonski, Phys. Rev. B **2013**, 88, 195427.

[33] J. Muñoz-García, L. Vazquez, M. Castro, R. Gago, A. Redondo-Cubero, A. Moreno-Barrado, R. Cuerno, Materials Science and Engineering R **2014**, 86, 1-44.

[34] R. Gago, L. Vazquez, F.J. Palomares, F. Agulló-Rueda, M. Vinnichenko, V. Carcelén, J. Olvera, J.L. Plaza, E. Diéguez, J. Phys. D: Appl. Phys. **2013**, 46, 455302.

[35] J. Shen, J. Kischner, Surf. Sci. **2002**, 500, 300.

[36] C. H. Sun, P. Jiang, B. Jiang. Appl. Phys. Lett. **2008**, 92, 061112.

[37] B. Kasemo, Surf. Sci. **2002**, 500, 656.

[38] A. Wellner, R.E. Palmer, J.G. Zheng, C.J. Kiely, K.W. Kolasinski, J. Appl. Phys. **2002**, 91(5) 3294.

[39] D. Datta, S.R. Bhattacharyya, T.K. Chini, M.K. Sanyal, Nucl. Instrum. Mathods Phys. Res. B **2002**, 193, 596.

[40] R. Alvarez, J.M. Garcia-Martin, M. Macias-Montero, L. Gonzalez-Garcia, J. C. Gonzalez, V. Rico, J. Perlich, J. Cotrino, A.R. Gonzalez-Elipe and A. Palmero, Nanotechnology **2013**, 24, 045604.

[41] J.A. Thornton, J. Vac. Sci. Technol. **1974**, 11, 666.

[42] J.A. Thornton, J. Vac. Sci. Technol. **1975**, 12, 830.

[43] K. van Aeken, SIMTRA, Available at http://www.draft.ugent.be/.

[44] K. van Aeken, S. Mahieu, D. Depla, J. Phys. D. Appl. Phys. **2008**, 41, 20530.

[45] The Software SRIM, Available at http://www.srim.org.

[46] M. Castro, R. Gago, R. Cuerno, J. Muñoz-Garcia and L. Vazquez, Physical Review B **2012**, 86, 214107.

[47] D. Necasand P. Klapetek, Cent. Eur. J. Phys. **2012**, 10, 181-188.

Figure caption

Figure 1.- Experimental setup and definition of the x axis of the patterned substrate.

Figure 2.- a) Cross-sectional images of simulated films grown on periodic patterned substrates ($\lambda = 80, 160$ cells and $A = 5, 25$ cells). Note that the substrate ripples appear with different color. b) Surface correlation length and roughness of these films as a function of thickness.

Figure 3.- Top views of simulated films grown on a flat substrate , a periodic patterned substrate with $\lambda = 80$ and $A = 25$ cells , a patterned substrate with fluctuating λ, with $\langle\lambda\rangle = 80$ and $A = 25$ cells, and a patterned substrate with fluctuating A, with $\lambda = 80$ and $\langle A\rangle = 25$ cells. The arrows indicate the incidence of the deposition flux.

Figure 4.- Oblivion Thickness as a function of substrate pattern amplitude and wavelength.

Figure 5.- a) Cross-sectional images of simulated films grown on patterned substrates (periodic substrate with $\lambda = 80$ and $A = 25$ cells, patterned substrate with fluctuating λ, with $\langle\lambda\rangle = 80$ and $A = 25$ cells, patterned substrate with fluctuating A, with $\lambda = 80$ and $\langle A\rangle = 25$ cells and a patterned substrate with fluctuating A and λ, with $\langle\lambda\rangle = 80$ and $\langle A\rangle = 25$ cells). Note that the substrate ripples are depicted with different color. b) Surface correlation length and roughness of these films as a function of thickness.

Figure 6.- Topography of the patterned substrate, as obtained by AFM (the ion beam irradiation to create the patterns was from top to bottom of the image). The arrow indicates the incidence of the deposition flux. A cross-sectional height profile in the direction of the arrow is also shown.

Figure 7.- a) Top view SEM images of the films grown on flat and patterned substrates as a function of thickness. The arrows indicate the incidence of the deposition flux. b) Correlation length and roughness as obtained from the surface topography of these films measured by AFM.

Figure 8.- a) Cross-sectional SEM image of the 1 μm thick thin film grown on the patterned substrate. The arrow indicates the incidence of the deposition flux. b) Cross-sectional STEM-HAADF image of the same film. The three stages of growth as a function of thickness are identified: for thicknesses below ~500 nm the film follows the substrate features in a Substrate Driven regime, while for thicknesses between ~500 and ~1000 nm columns merge and form large structures in a typical Columnar Aggregation regime. Finally, for thicknesses above ~1000 nm, columns develop independent of substrate features in a typical Free Growth regime.

TABLE OF CONTENTS

The influence of substrate patterns on the nanocolumnar growth of SiO_2 thin films at oblique angles is studied. A critical thickness has been determined, below which the columnar growth is modulated by the substrate topography. For thicknesses above, pattern height fluctuations are responsible for the appearance of large tilted structures that grow independent of substrate features.

Fig 1

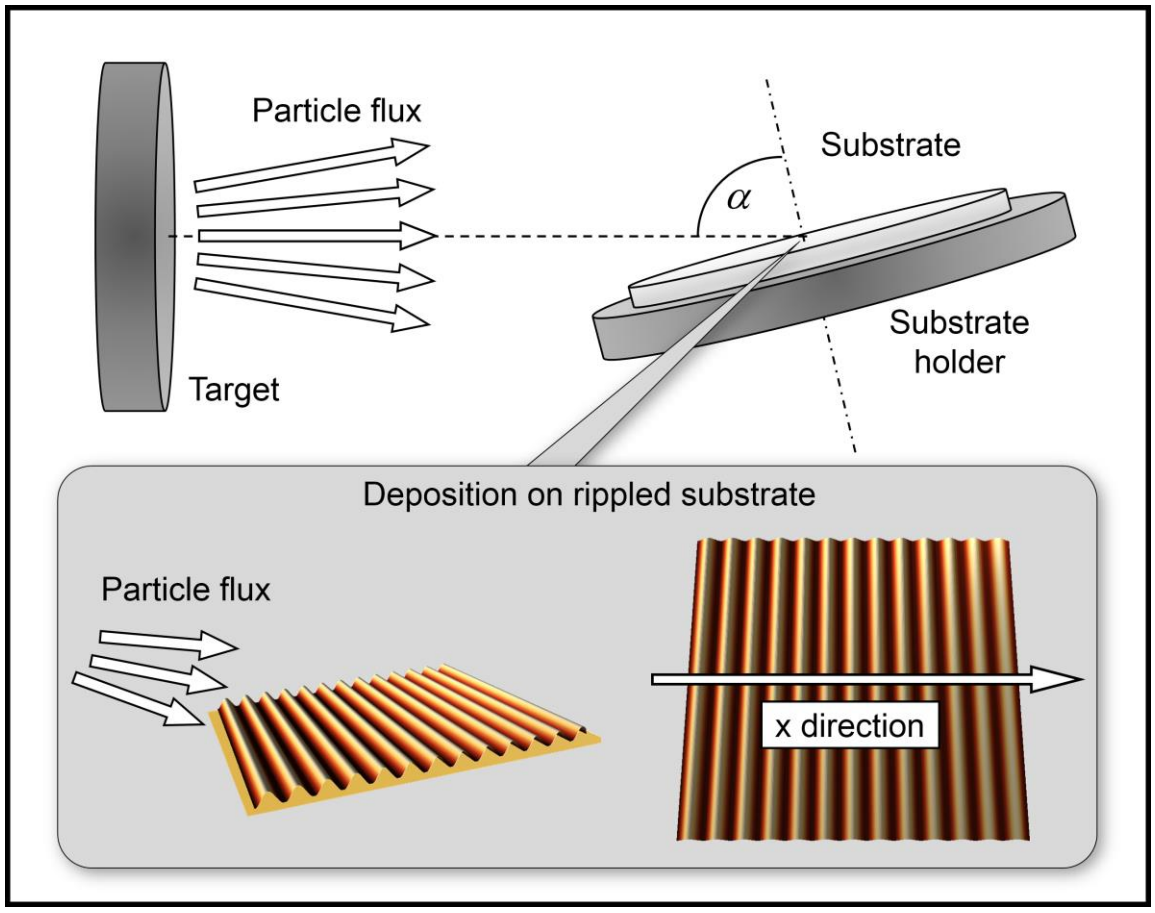
Particle flux
Target
Substrate
α
Substrate holder
Deposition on rippled substrate
Particle flux
x direction

Fig 2

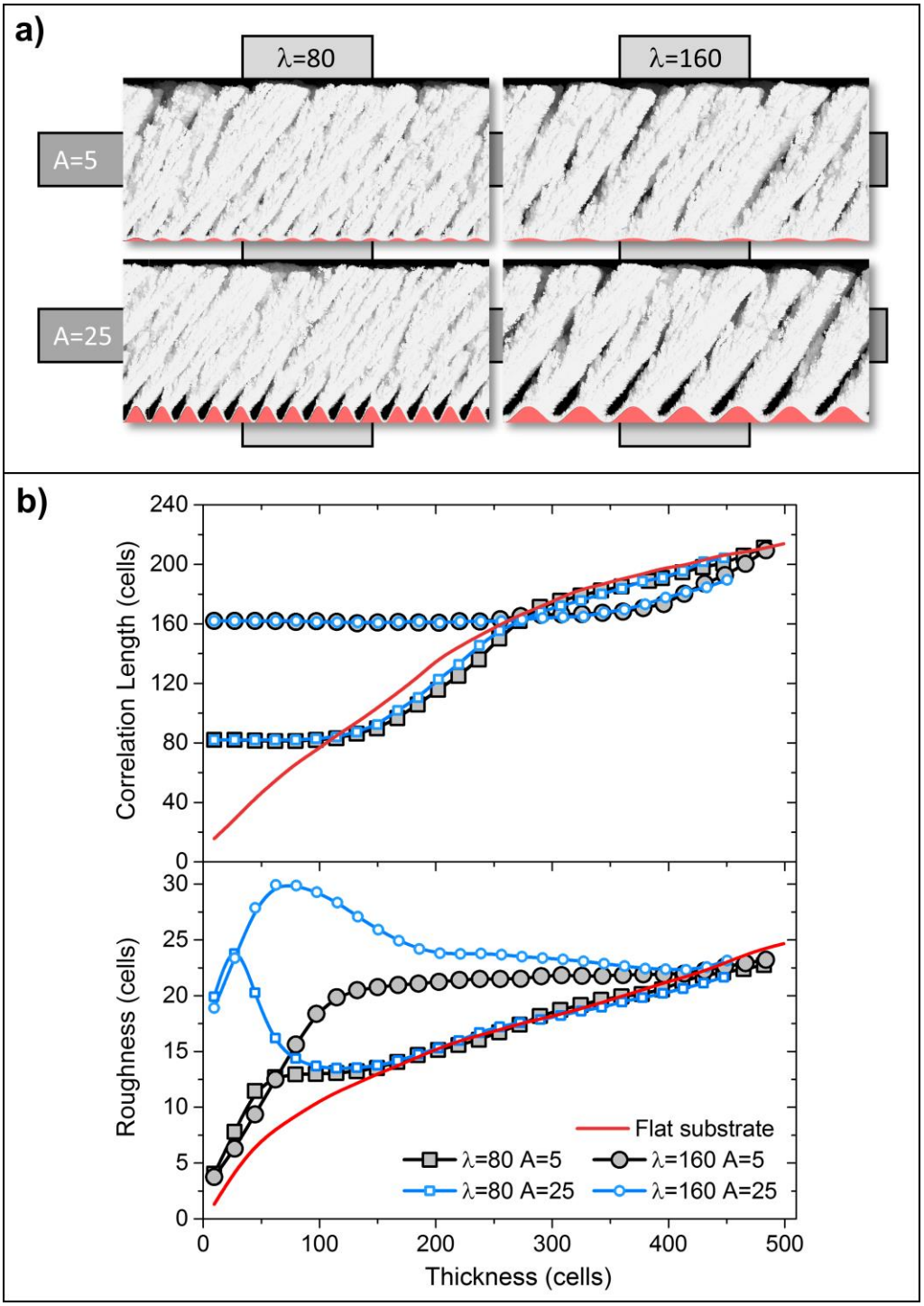
a)
λ=80
λ=160
A=5
A=25
b)
Correlation Length (cells)
Roughness (cells)
Thickness (cells)
Flat substrate
λ=80 A=5
λ=160 A=5
λ=80 A=25
λ=160 A=25

Fig 3

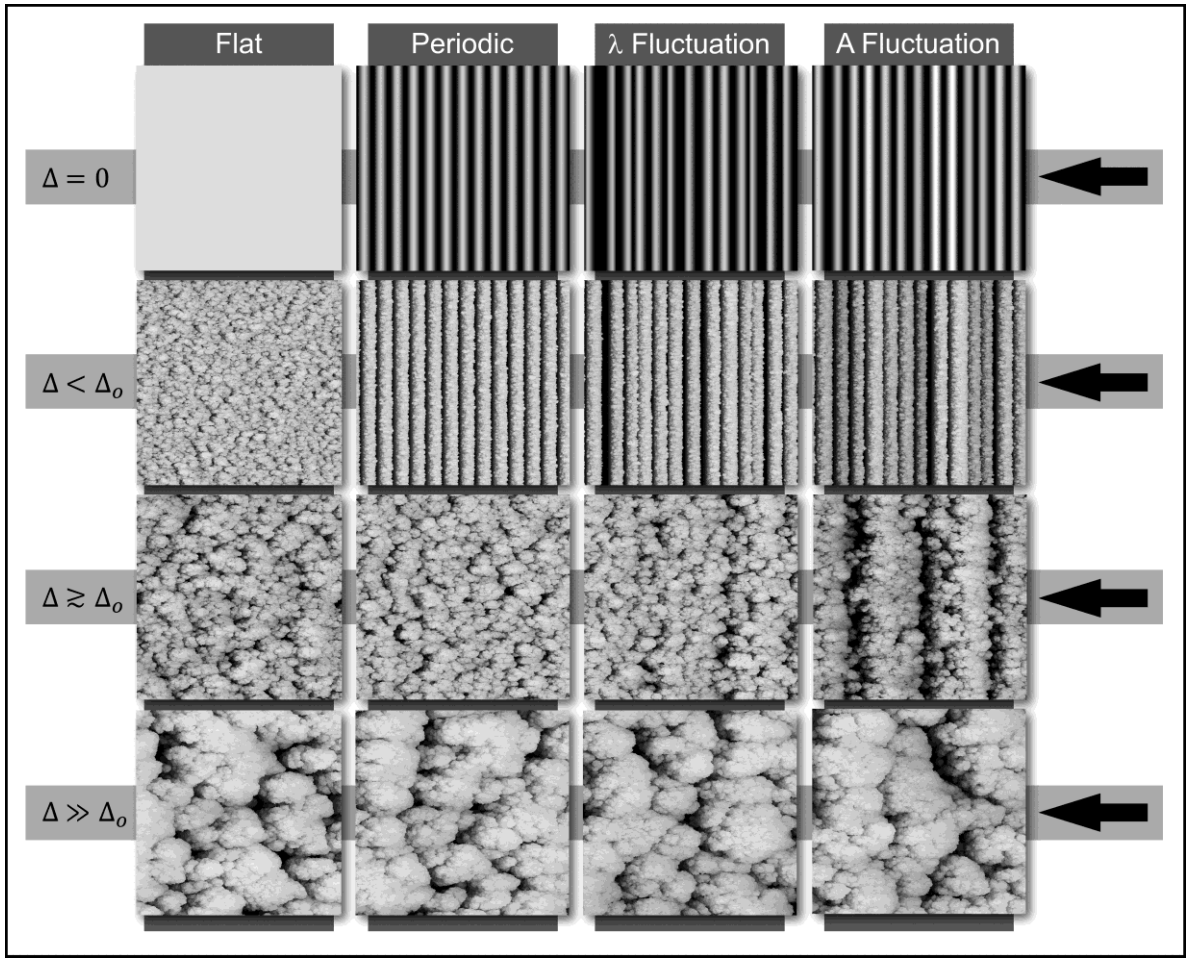
Flat
Periodic
λ Fluctuation
A Fluctuation
$\Delta = 0$
$\Delta < \Delta_o$
$\Delta \gtrsim \Delta_o$
$\Delta \gg \Delta_o$

Fig 4

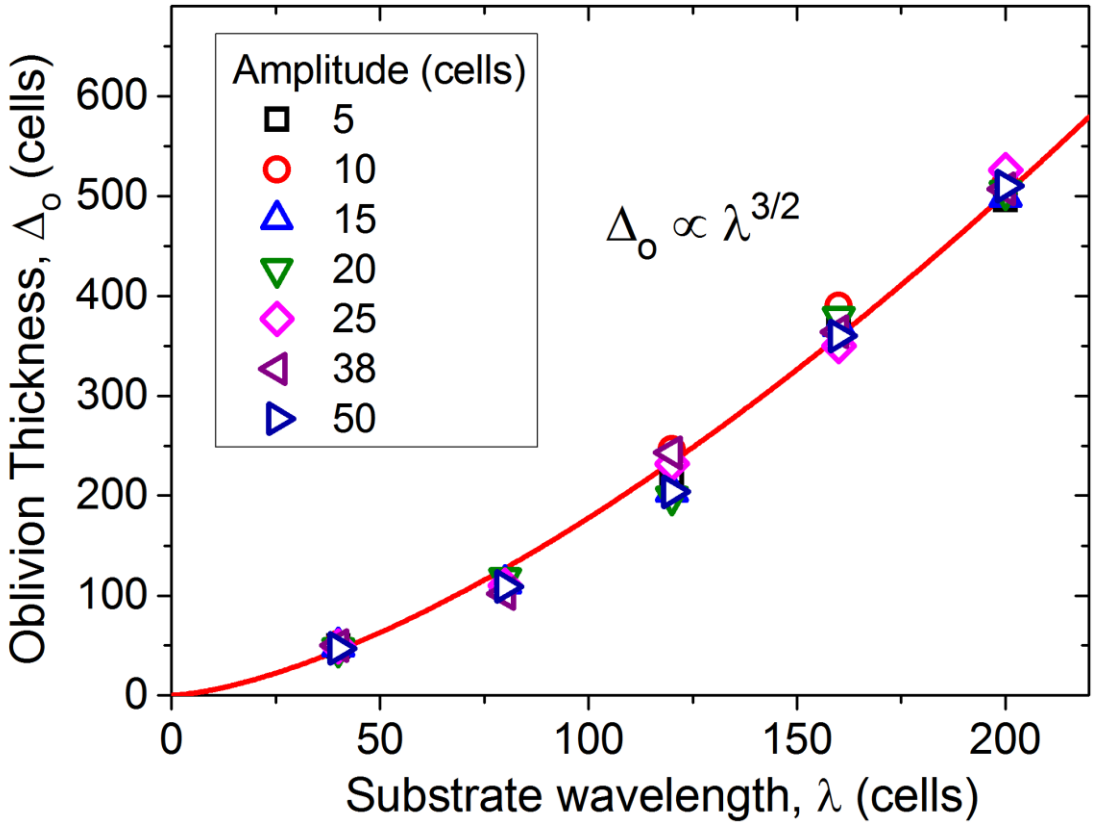
Amplitude (cells)
5
10
15
20
25
38
50
$\Delta_o \propto \lambda^{3/2}$
Oblivion Thickness, Δ_o (cells)
Substrate wavelength, λ (cells)
0
100
200
300
400
500
600
0
50
100
150
200

Fig 5

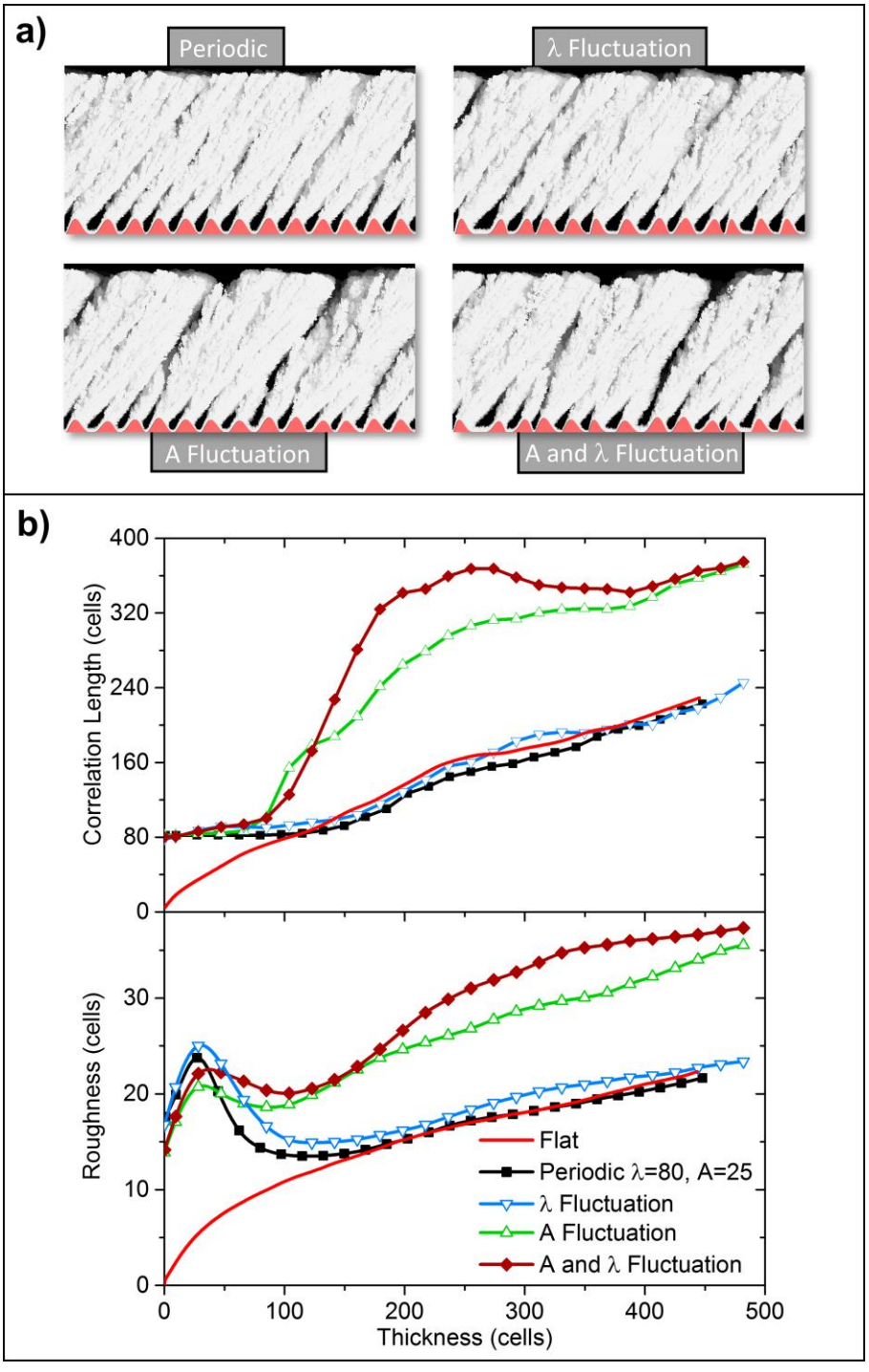
a)
Periodic
λ Fluctuation
A Fluctuation
A and λ Fluctuation
b)
Correlation Length (cells)
Roughness (cells)
Thickness (cells)
Flat
Periodic λ=80, A=25
λ Fluctuation
A Fluctuation
A and λ Fluctuation

Fig 6

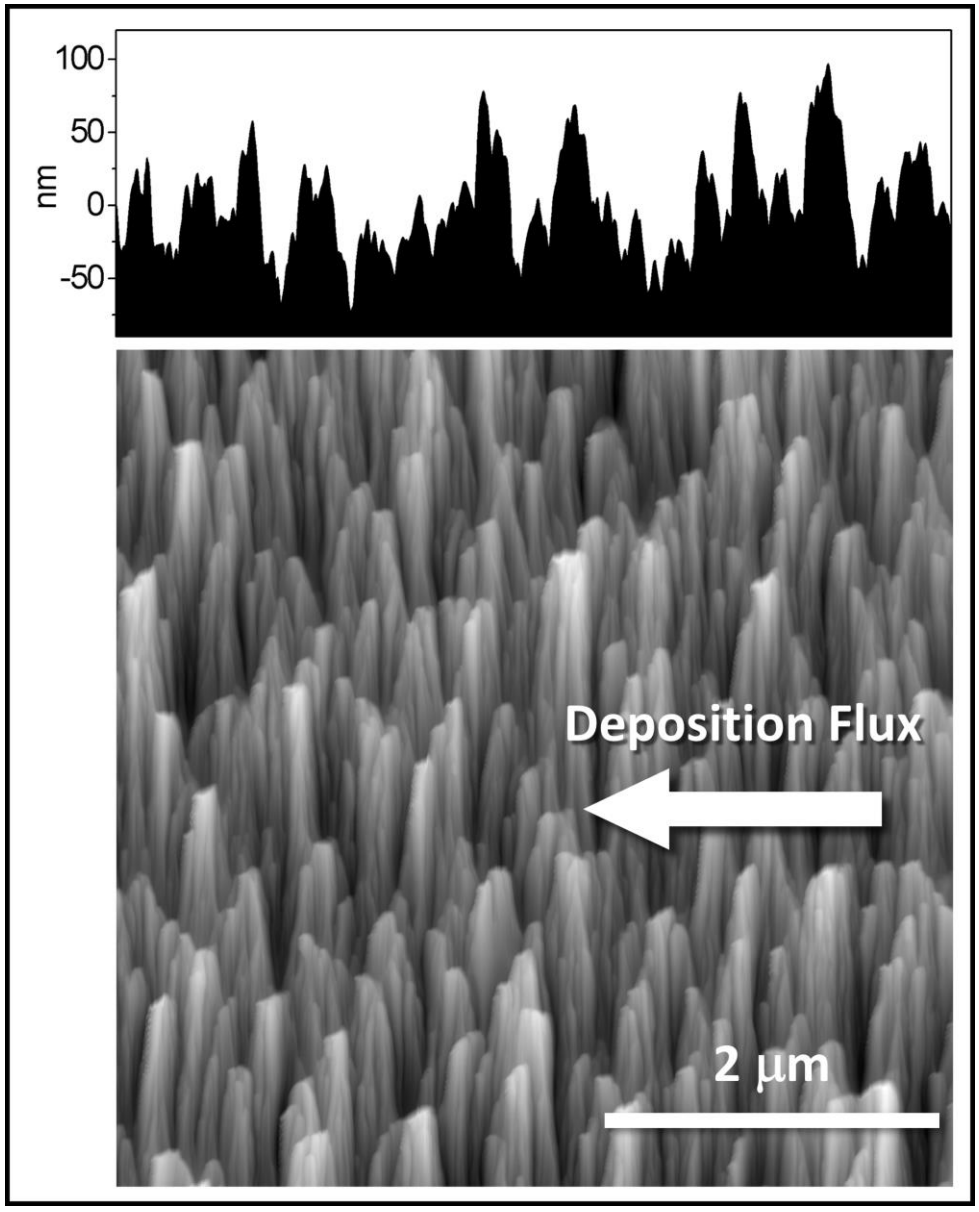

Fig 7

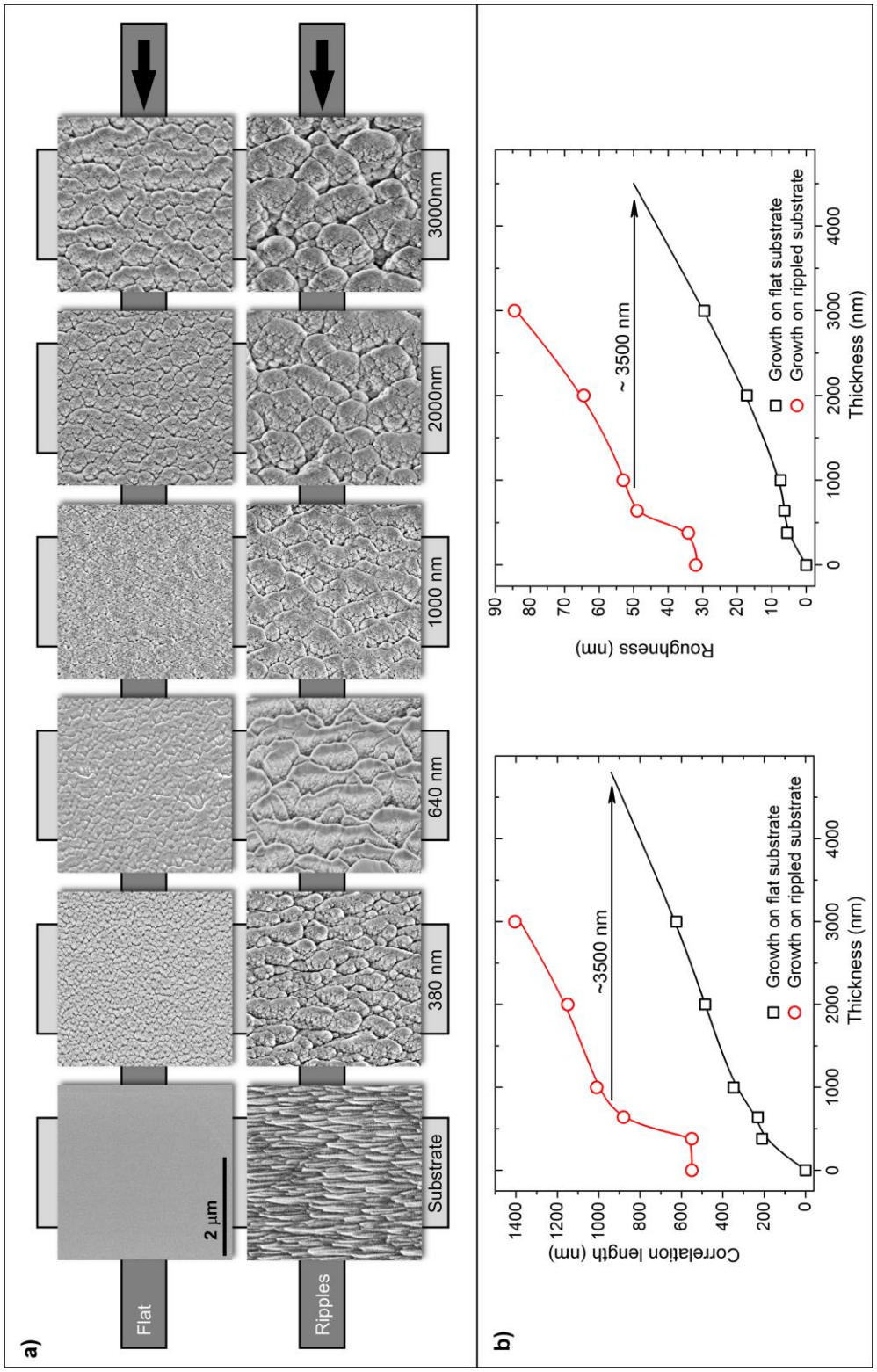
a)
Flat
Ripples
2 µm
Substrate
380 nm
640 nm
1000 nm
2000nm
3000nm
b)
Correlation length (nm)
~3500 nm
Growth on flat substrate
Growth on rippled substrate
Thickness (nm)
Roughness (nm)
~ 3500 nm
Growth on flat substrate
Growth on rippled substrate
Thickness (nm)

Fig 8

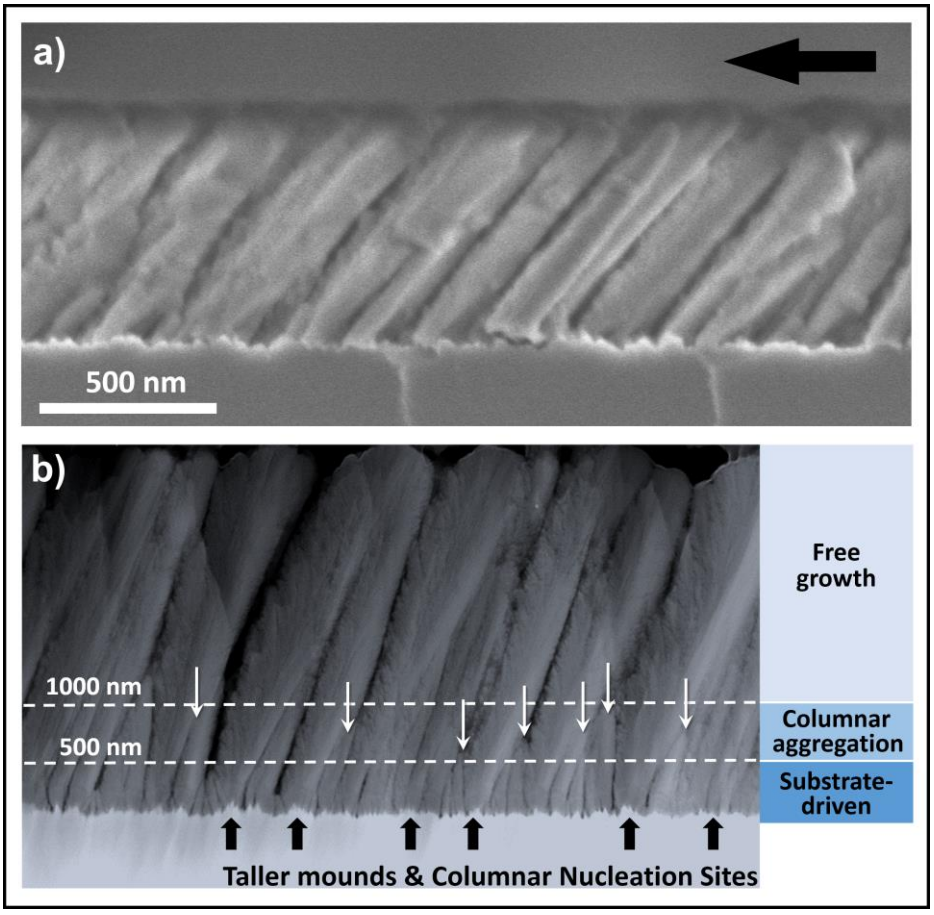
a)
500 nm
b)
Free growth
1000 nm
Columnar aggregation
500 nm
Substrate-driven
Taller mounds & Columnar Nucleation Sites